Krabbe disease successfully treated via monotherapy of intrathecal gene therapy

Allison M. Bradbury,[1] Jessica H. Bagel,[1] Duc Nguyen,[2] Erik A. Lykken,[3] Jill Pesayco Salvador,[4] Xuntian Jiang,[5] Gary P. Swain,[1] Charles A. Assenmacher,[6] Ian J. Hendricks,[1] Keiko Miyadera,[1] Rebecka S. Hess,[1] Arielle Ostrager,[1] Patricia ODonnell,[1] Mark S. Sands,[5] Daniel S. Ory,[5] G. Diane Shelton,[4] Ernesto R. Bongarzone,[2] Steven J. Gray,[3] and Charles H. Vite[1]

[1]Department of Clinical Sciences and Advanced Medicine, School of Veterinary Medicine, University of Pennsylvania, Philadelphia, Pennsylvania, USA. [2]Department of Anatomy and Cell Biology, College of Medicine, University of Illinois at Chicago, Chicago, Illinois, USA. [3]Department of Pediatrics, University of Texas Southwestern Medical Center, Dallas, Texas, USA. [4]Department of Pathology, School of Medicine, University of California San Diego, La Jolla, California, USA. [5]Department of Medicine, Washington University School of Medicine, St. Louis, Missouri, USA. [6]Department of Pathobiology, School of Veterinary Medicine, University of Pennsylvania, Philadelphia, Pennsylvania, USA.

Globoid cell leukodystrophy (GLD; Krabbe disease) is a progressive, incurable neurodegenerative disease caused by deficient activity of the hydrolytic enzyme galactosylceramidase (GALC). The ensuing cytotoxic accumulation of psychosine results in diffuse central and peripheral nervous system (CNS, PNS) demyelination. Presymptomatic hematopoietic stem cell transplantation (HSCT) is the only treatment for infantile-onset GLD; however, clinical outcomes of HSCT recipients often remain poor, and procedure-related morbidity is high. There are no effective therapies for symptomatic patients. Herein, we demonstrate in the naturally occurring canine model of GLD that presymptomatic monotherapy with intrathecal AAV9 encoding canine GALC administered into the cisterna magna increased GALC enzyme activity, normalized psychosine concentration, improved myelination, and attenuated inflammation in both the CNS and PNS. Moreover, AAV-mediated therapy successfully prevented clinical neurological dysfunction, allowing treated dogs to live beyond 2.5 years of age, more than 7 times longer than untreated dogs. Furthermore, we found that a 5-fold lower dose resulted in an attenuated form of disease, indicating that sufficient dosing is critical. Finally, postsymptomatic therapy with high-dose AAV9 also significantly extended lifespan, signifying a treatment option for patients for whom HSCT is not applicable. If translatable to patients, these findings would improve the outcomes of patients treated either pre- or postsymptomatically.

Introduction

Globoid cell leukodystrophy (GLD; Krabbe disease, OMIM 245200), a hereditary disorder due to mutations in the *GALC* gene, is characterized by deficiency of the hydrolytic lysosomal enzyme galactosylceramidase (GALC), which catabolizes the major myelin lipid galactosylceramide during normal myelin turnover (1). In the infantile form of GLD, undigested galactosylceramide accumulation in macrophages results in globoid cell formation in the central nervous system (CNS), and galactolipid inclusions are accumulated in histiocytes in the peripheral nervous system (PNS). GALC is also responsible for the degradation of galactosylsphingosine (psychosine), an intermediate in the biosynthesis of cerebrosides. Cytotoxic accumulation of psychosine in oligodendrocytes in GLD causes cell death. The abnormal turnover of myelin and the death of oligodendrocytes compromise normal myelination in the developing infant, leading to irritability, paresis/paralysis, hearing loss, blindness, decerebration, and death by 2 years of age (2–5). Presymptomatic hematopoietic stem cell transplantation (HSCT) is the only treatment for infantile GLD; however, long-term outcomes of transplanted patients remain poor, and morbidity associated with the procedure is high (5–9). Moreover, HSCT does not treat the PNS disease associated with GLD (5–9). HSCT is no longer indicated for postsymptomatic patients.

Naturally occurring canine GLD is due to a spontaneous missense mutation in the *GALC* gene, c.473A>C (10), and disease progression in GLD dogs closely recapitulates human disease (10–14). The predictable disease progression (onset of neurological dysfunction at 6 weeks of age) and lifespan (15.7 ± 4.8 weeks of age) (12) allow for timely identification of pathological changes and evaluation of therapeutic interventions. Intrathecal delivery of adeno-associated virus serotype 9 (AAV9) encoding murine GALC to postsymptomatic twitcher mice, a naturally occurring murine model of Krabbe disease, modestly extended lifespan from 40 to 50.5 days, improved pathology, and partially reduced psychosine levels (15). We undertook a similar strategy in both presymptomatic and postsymptomatic GLD dogs, an animal model with a gyrencephalic brain more similar in size to an infant's brain. Herein we demonstrate that a

Conflict of interest: AMB is a beneficiary of a licensing agreement with Axovant Gene Therapies (royalties). DSO is an employee of and has equity holdings in Casma Therapeutics. ERB has received income from E-Scape Bio and Lysosomal Therapeutics Inc. (consulting). SJG has received research funding from Neurogene and Abeona and has received income from Neurogene (consulting and royalties) and Vertex Pharmaceuticals (consulting). CHV has received research funding from BioMarin Pharmaceuticals. SJG, EAL, CHV, and AMB are inventors on a patent pending related to the GALC vector: Optimized GALC Genes and Expression Cassettes and Their Use (PCT/US2019/067727).

Submitted: October 1, 2019; **Accepted:** June 4, 2020; **Published:** August 10, 2020.
Reference information: *J Clin Invest*. 2020;130(9):4906–4920.
https://doi.org/10.1172/JCI133953.

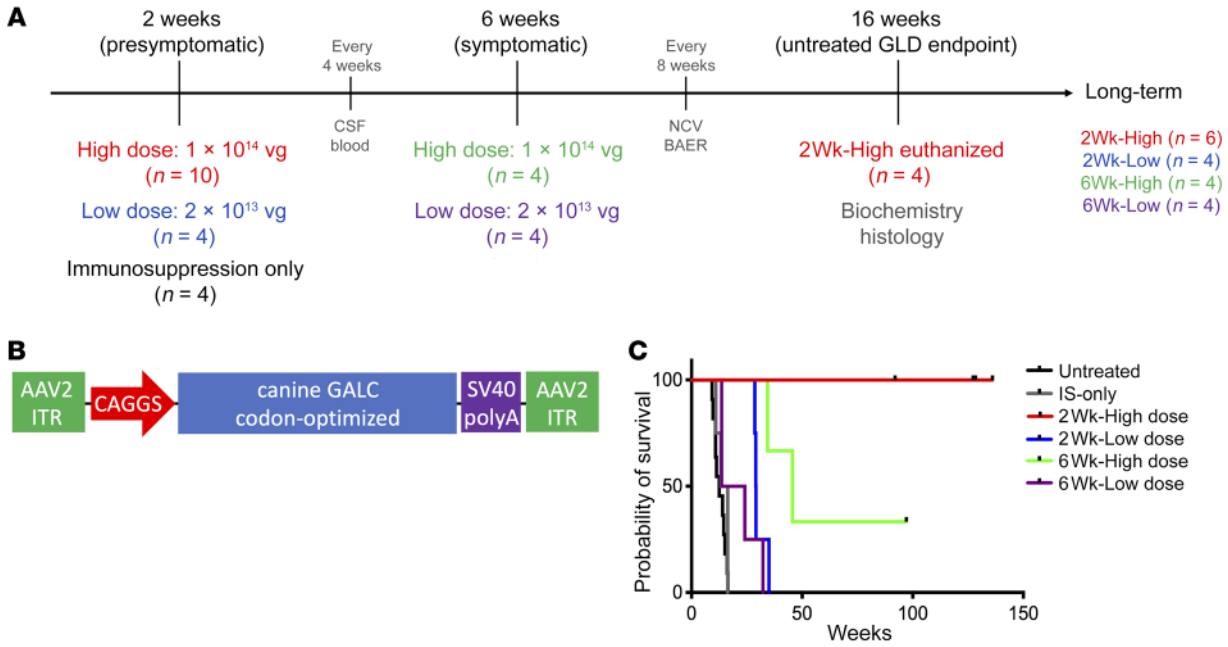

Figure 1. Experimental design, vector construct, and survival. (**A**) GLD dogs were treated with AAV9 delivered to the cisterna magna in a 1-mL volume. Ten GLD dogs were treated at 2 weeks of age with 1×10^{14} vg (2Wk-High); 4 GLD dogs were treated at 2 weeks of age with 2×10^{13} vg (2Wk-Low); 4 GLD dogs were treated at 6 weeks of age with 1×10^{14} vg (6Wk-High); 4 GLD dogs were treated at 6 weeks of age with 2×10^{13} vg (6Wk-Low). All dogs received an immunosuppression protocol consisting of 20 mg/kg intravenous methylprednisolone 1 hour before AAV infusion followed by 4 months of daily oral prednisone (0.5 mg/kg) with a 2-week taper. Four GLD dogs received immunosuppression protocol alone (IS-only). Four 2Wk-High dogs were euthanized at a predetermined endpoint of 16 weeks, while the remaining 22 dogs were followed long-term. (**B**) The AAV9 construct consisted of inverted terminal repeats (ITR), a CAGGS promoter, a codon-optimized canine *GALC* transgene, and a polyadenylation signal. (**C**) Percentage survival of untreated GLD (black), IS-only (gray), 2Wk-High (red), 2Wk-Low (blue), 6Wk-High (green), and 6Wk-Low (purple). A drop in the line indicates a death due to disease progression, and a black tick mark indicates dogs still alive ($n = 1$ in the 6Wk-High cohort, $n = 6$ in the 2Wk-High cohort). NCV, nerve conduction velocity testing; BAER, brainstem auditory evoked response testing.

single intrathecal injection at the cisterna magna (intracisternal) of AAV9 encoding canine GALC (AAV9-cGALC) was capable of clinically, biochemically, and histologically amending both CNS and PNS disease, delaying the onset of neurological dysfunction and prolonging survival. In fact, presymptomatic delivery of high-dose AAV increased lifespan to more than 7 times that of untreated GLD dogs, with all treated dogs remaining neurologically normal beyond 1.5 years of age. Moreover, in this robust evaluation of 26 GLD dogs, we demonstrate that this intracisternal protocol is sufficient to globally deliver therapeutic GALC enzyme, reduce cytotoxic psychosine concentrations, and correct the myelination abnormalities present in both the CNS and PNS. Importantly, this therapy obviates the need for HSCT. Furthermore, our data in the canine GLD model confirm a positive effect in dogs treated postsymptomatically, an improvement that has not been described in pediatric patients with HSCT. Last, the minimal effective dose determined in the canine model should inform translation of intrathecal AAV9 gene therapy into the clinic for the treatment of Krabbe disease.

Results

Pre- or postsymptomatic intracisternal administration of 1×10^{14} vector genomes of AAV9-cGALC to GLD dogs mitigates neurological dysfunction. Four cohorts of GLD dogs were injected intrathecally at the cisterna magna with AAV9 encoding canine GALC driven by a CAGGS promoter, which combines the cytomegalovirus (CMV) early enhancer element with the chicken β-actin promoter (AAV9-cGALC; Figure 1, A and B). All AAV9-treated dogs received prednisone at an immunosuppressive dose immediately before and for 4 months after injection. Two cohorts of GLD dogs were treated presymptomatically at 2 weeks of age with either a high dose of vector (2Wk-High, receiving 1×10^{14} vector genomes [vg], $n = 10$) or a lower dose (2Wk-Low, receiving 2×10^{13} vg, $n = 4$). All 2-week-old GLD dogs were neurologically normal at the time of injection. The remaining 2 cohorts were treated postsymptomatically at 6 weeks of age, again with either a high dose (6Wk-High, receiving 1×10^{14} vg, $n = 4$) or a low dose of vector (6Wk-Low, receiving 2×10^{13}, $n = 4$). All 6-week-old GLD dogs exhibited tremors and pelvic limb weakness at the time of injection. Dogs either were euthanized at 16 weeks of age, the mean age of death of untreated GLD dogs, or were followed long-term. A control cohort of GLD dogs that received immunosuppression regimen alone (IS-only) was also evaluated (Figure 1A).

Untreated GLD dogs developed tremors and pelvic limb weakness at 6 weeks of age and progressed to pelvic limb ataxia, thoracic limb dysmetria, and urinary incontinence. Endpoint disease, defined as pelvic limb paralysis, occurred at 15.7 ± 4.8 weeks of age (12). GLD dogs in the IS-only cohort showed a disease progression indistinguishable from that of untreated GLD dogs with endpoint disease occurring between 11.0 and 16.4 weeks of age (14.29 ± 2.29 weeks; $P = 0.2954$) (Supplemental Video 1, IS-only dog at 10 weeks of age; supplemental material available online with this article; https://doi.org/10.1172/JCI133953DS1). There was no evidence that GLD dogs showed any benefit from IS alone.

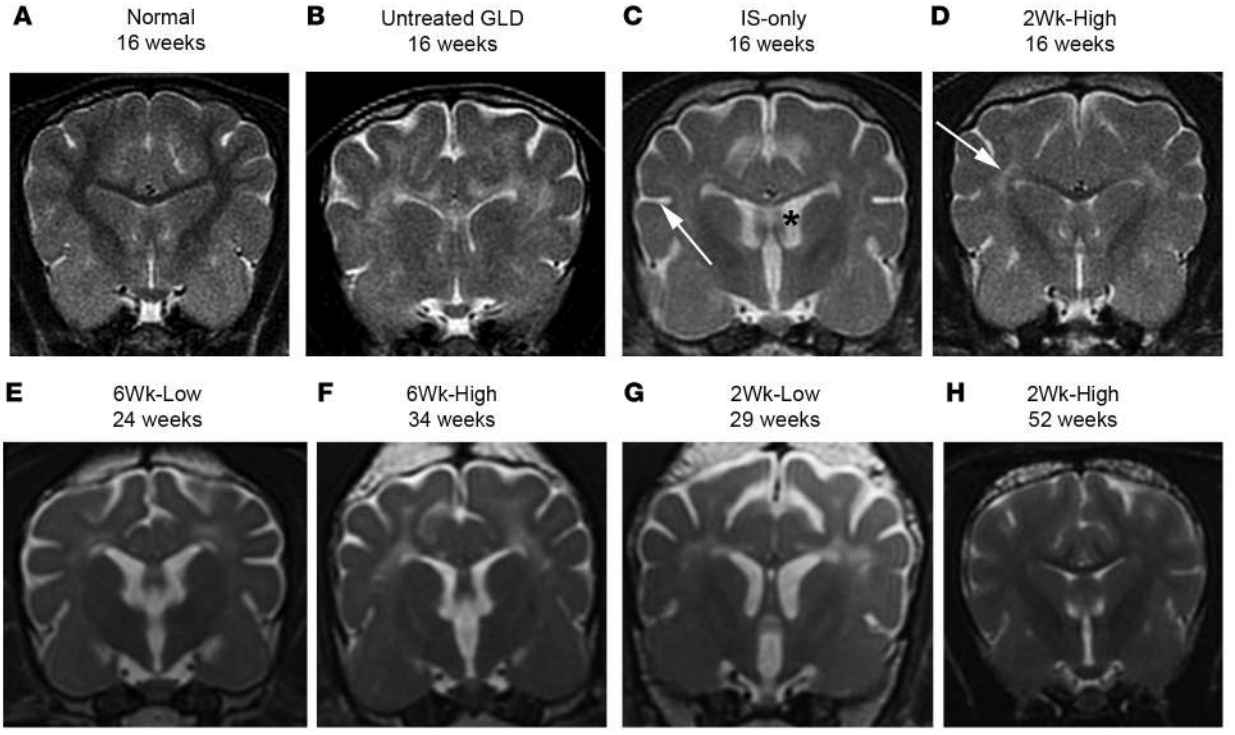

Figure 2. MRI of the brain at 1.5T. T2-weighted images at the level of the caudate nucleus in a normal dog at 16 weeks of age (**A**), an untreated GLD dog at endpoint (16 weeks of age) (**B**), IS-only at endpoint (16 weeks of age) (**C**), 2Wk-High at 16 weeks of age (**D**), 6Wk-Low at endpoint (24 weeks of age) (**E**), 6Wk-High at endpoint (34 weeks of age) (**F**), 2Wk-Low at endpoint (29 weeks of age) (**G**), and 2Wk-High at 52 weeks of age (**H**). White arrow in **C** indicates widened sulcus; black asterisk in **C** indicates enlarged ventricle. White arrow in **D** indicates hyperintensity of the centrum semiovale relative to gray matter.

Remarkably, all 10 GLD dogs in the 2Wk-High cohort were clinically normal at 16 weeks of age. Four dogs in this cohort were euthanized for biochemical and histological evaluation of tissues at 16 weeks of age, with results presented below. Six of these dogs, which are being evaluated long-term, remain neurologically normal and are currently all over 1.5 years of age (136.0, 128.4, 127.3, 127.3, 92.0, and 92.0 weeks of age) (Supplemental Video 2, GLD 2Wk-High at 116 weeks of age; and Figure 1C).

In contrast to the 2Wk-High cohort, each of the 4 dogs in the 2Wk-Low cohort developed pelvic limb ataxia by 16 weeks of age but remained able to walk. In order to evaluate disease progression in this cohort, no dogs were euthanized at 16 weeks of age and all were followed long-term. Three of 4 dogs developed behavioral abnormalities (disorientation and anxiety) and postretinal (central) blindness by 25 weeks of age. On ophthalmic examination, the fundus, retina, and optic disc appeared structurally normal (Supplemental Figure 1, C and F). Intriguingly, behavioral changes and blindness were not identified in any dogs in the untreated GLD or IS-only cohorts. Endpoint disease, defined as (a) severe disorientation with blindness (n = 3) and/or (b) pelvic limb paralysis (n = 2), occurred at 28.6–35.0 weeks of age (P = 0.0002 vs. IS only; 30.43 ± 2.65 weeks, n = 4) (Supplemental Video 3, GLD 2Wk-Low at 27 weeks of age; and Figure 1C).

Assessment of the effect of administration of AAV9-cGALC to 6-week-old GLD dogs with signs of neurological dysfunction revealed that postsymptomatic therapy was less effective than presymptomatic therapy at the respective doses evaluated. Of the 4 dogs in the 6Wk-High cohort, 2 developed pelvic limb paralysis at 34.4 and 45.6 weeks of age. One dog in this cohort is currently 97.1 weeks of age and shows mild pelvic limb ataxia. The remaining dog in this cohort was euthanized at 17 weeks of age owing to severe bilateral patellar luxations that limited its ability to walk. This confounding orthopedic abnormality is not associated with GLD. GLD dogs in the 6Wk-Low cohort fared worse than the 6Wk-High cohort. All 4 dogs were euthanized between 13.6 and 32.3 weeks of age (20.89 ± 7.66 weeks, n = 4) owing to pelvic limb paralysis; survival time was not significantly different (P = 0.2425) from that of GLD dogs that received IS only.

MRI of the brain shows global amelioration of myelination abnormalities and atrophy in GLD dogs treated presymptomatically with 1×10^{14} vg AAV9-cGALC. On T2-weighted images, all 16-week-old untreated GLD dogs showed bilaterally symmetrical hyperintensities, relative to gray matter, of the corona radiata, corpus callosum, centrum semiovale, internal capsule (Figure 2B), and cerebellar white matter (not shown) when compared with normal, age-matched control dogs (Figure 2A). These changes are consistent with loss of myelin. Furthermore, brain atrophy, characterized by cerebral ventricular dilation and widened sulci, was also seen in untreated GLD dogs (Figure 2B). Imaging results of IS-only dogs at endpoint were indistinguishable from those of untreated GLD dogs showing diffuse white matter hyperintensity (Supplemental Table 1, MRI) as well as widened sulci (Figure 2C, arrow) and enlarged ventricles (Figure 2C, asterisk).

Dogs in the 2Wk-High cohort (Figure 2D) showed white matter signal intensities more similar to those of normal dogs (Figure 2A). The following white matter structures were normal (hypointense

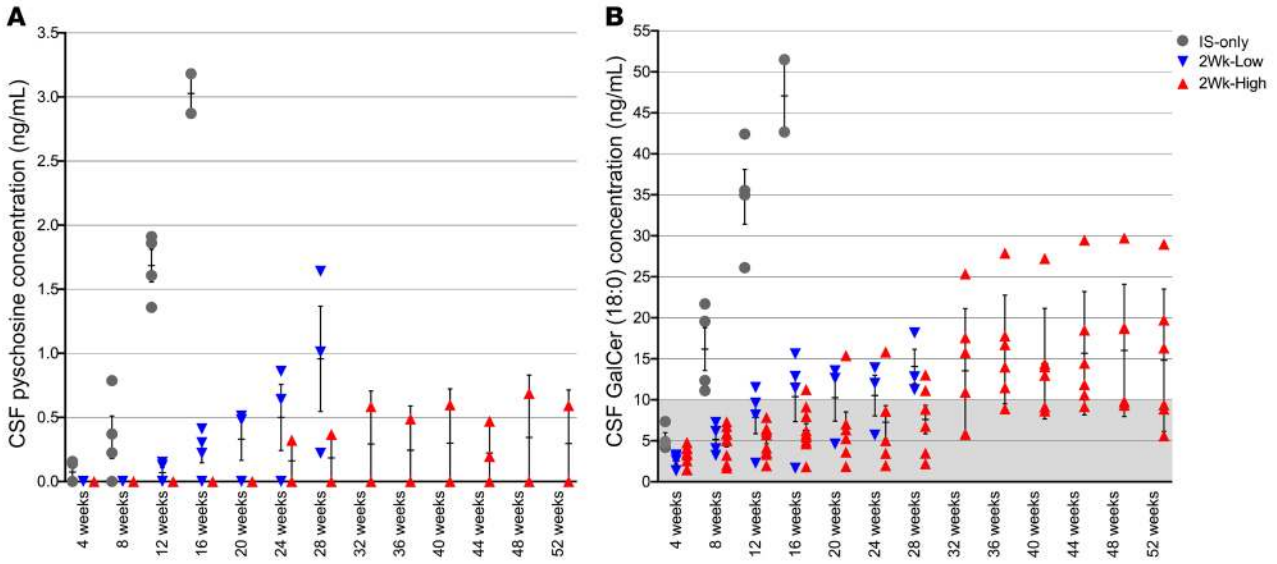

Figure 3. CSF concentrations of psychosine and galactosylceramide. Psychosine (**A**) and galactosylceramide (GalCer) (**B**) were measured by mass spectrometry every 4 weeks up to 52 weeks of age. Psychosine and GalCer are reported in ng/mL. Psychosine was below the level of detection in normal dogs. Gray shading indicates normal range for canine samples collected at the cisterna magna (<10 ng/mL) for GalCer. IS-only (n = 4, gray circles), 2Wk-High (n = 10, ≤16 weeks of age; n = 6, >16 weeks of age; red triangles), 2Wk-Low (n = 4, ≤16 weeks of age; n = 3, >16 weeks of age; blue triangles). Lines represent mean with SEM. Nonparametric Kruskal-Wallis test and Mann-Whitney test were performed. A P value of less than 0.05 was considered significant.

relative to gray matter) at 16 weeks of age: corona radiata in 2/4 dogs; corpus callosum in 4/4 dogs; centrum semiovale in 1/4 dogs; internal capsule in 3/4 dogs; and cerebellar white matter in 4/4 dogs (Supplemental Table 1, MRI). At 52 weeks of age, white matter signal intensities were normal in the corona radiata (4/6 dogs), corpus callosum (5/6 dogs), centrum semiovale (1/6 dogs), internal capsule (4/6 dogs), and cerebellar white matter (6/6 dogs) (Figure 2H). In the 2Wk-Low cohort at endpoint (Figure 2G), signal intensity was normal in the cerebellum, the brain region nearest the injection site, in 3/4 dogs; normalization of white matter signal intensity did not occur in the corona radiata, centrum semiovale, or internal capsule in any dog. The dog in this cohort that did not develop behavioral abnormalities or blindness was the dog with the least white matter signal abnormalities, including normal signal intensity in the corpus callosum and the occipital radiations. In contrast to the other cohorts, all dogs (4/4) in the 2Wk-Low cohort at endpoint showed gadolinium enhancement diffusely throughout the cerebral white matter including the optic radiations, suggesting an inflammatory phase of disease progression (Supplemental Figure 1, A and D, and Supplemental Table 1, MRI).

In the postsymptomatic cohorts (Figure 2, E and F), white matter signal intensity was similar to that in untreated dogs. Normalization of the white matter signal intensity was observed in the corpus callosum of 2/7 dogs and in the cerebellar white matter of 2/7 dogs but was not seen in any other brain region analyzed (Supplemental Table 1).

For all cohorts, the white matter that showed the most signal abnormalities was the centrum semiovale. As this is an initiating point for pathology in Krabbe disease, it is plausible that lesions were present in the centrum semiovale at the time of treatment. It is interesting to note that in the 2Wk-High cohort signal abnormalities in the centrum semiovale remained stable from 16 to 52 weeks.

In order to quantify brain atrophy, the areas of the mass intermedia and of the cerebellum were determined on mid-sagittal images. The mass intermedia area of the 2Wk-High cohort was not different from normal (P = 0.624) and was significantly larger than those of the untreated GLD (P = 0.012), 2Wk-Low (P = 0.005), and 6Wk-High (P = 0.011) cohorts. The 2Wk-Low (P = 0.011), 6Wk-High (P = 0.020), and 6Wk-Low (P = 0.011) cohorts all had mass intermedia areas significantly smaller than that of normal dogs. The cerebellar areas of both the 2Wk-High and 2Wk-Low cohorts were not different from normal (P = 0.741, P = 0.321) and were significantly larger than that of untreated GLD dogs (P = 0.010, P = 0.046). Both postsymptomatic cohorts were not significantly different from normal or untreated GLD dogs (P > 0.05), suggesting an intermediate level of correction. These findings demonstrate substantial attenuation of brain atrophy with presymptomatic high-dose treatment, but not with low-dose or delayed treatment.

Cerebrospinal fluid psychosine, galactosylceramide, and total protein concentrations are normalized in GLD dogs treated presymptomatically with 1 × 10^{14} vg AAV9-cGALC. Similar to recent findings in untreated GLD dogs (16), cerebrospinal fluid (CSF) psychosine concentrations were elevated in IS-only dogs at 4 weeks of age and increased with disease progression (Figure 3A). Psychosine was not detectable in the CSF of normal dogs at any time point. In the 2Wk-High cohort, psychosine was not detectable in any treated animal up to 20 weeks of age; at 24 weeks of age, psychosine was detectable in 1 of 6 dogs, and it remained relatively stable beyond 32 weeks of age. Psychosine was also detectable at a single time point, 44 weeks of age, in a second dog of this cohort (Figure 3A). Psychosine concentrations were significantly reduced as compared with IS-only at 4 (P = 0.020), 8 (P = 0.003), and 12 (P = 0.0004) weeks and were not significantly different (P > 0.05) from those in

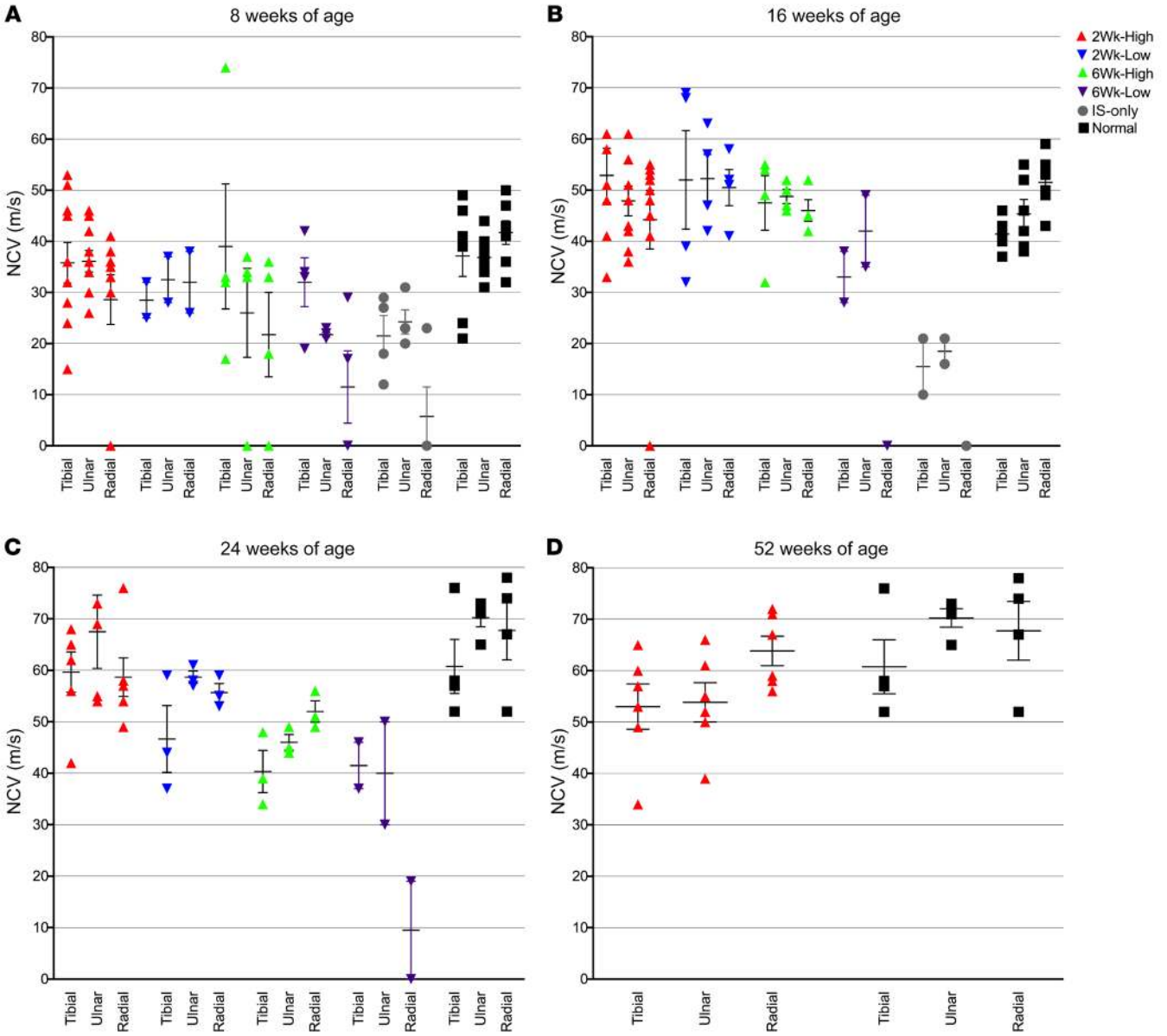

Figure 4. Motor and sensory nerve conduction velocities at 8, 16, 24, and 52 weeks of age. The motor nerve conduction velocities (NCVs) of the tibial and ulnar nerves and the sensory NCVs of the radial nerves were analyzed at 8 weeks of age for normal (n = 7, black squares), 2Wk-High (n = 10, red triangles), 2Wk-Low (n = 2, blue triangles), 6Wk-High (n = 4, green triangles), 6Wk-Low (n = 4, purple triangles), and IS-only (n = 4, gray circles) (**A**); 16 weeks of age for normal (n = 6), 2Wk-High (n = 9), 2Wk-Low (n = 4), 6Wk-High (n = 4), and 6Wk-Low (n = 2) (**B**); 24 weeks of age for normal (n = 6), 2Wk-High (n = 6), 2Wk-Low (n = 3), 6Wk-High (n = 3), and 6Wk-Low (n = 2) (**C**); and 52 weeks of age for normal (n = 4) and 2Wk-High (n = 6) (**D**). Lines represent mean with SEM. Nonparametric Kruskal-Wallis test and Mann-Whitney test were performed. A P value of less than 0.05 was considered significant.

normal age-matched controls at any time point (Supplemental Table 1). In the 2Wk-Low cohort, the accumulation of psychosine was delayed until 12 weeks of age and increased steadily in all dogs until endpoint (Figure 3A). The levels remained significantly lower than in IS-only dogs at 8 (P = 0.0472) and 12 (P = 0.0202) weeks of age. The 2Wk-High cohort was significantly lower than the 2Wk-Low cohort from 12 weeks (P = 0.0203) to 28 weeks of age (P = 0.0237). These data identify CSF psychosine as a robust, disease-specific biomarker of disease severity and therapeutic efficacy.

The natural substrate of GALC, galactosylceramide (GalCer), was also significantly elevated in CSF of untreated GLD dogs, and 18:0 was determined to be the most abundant species (16). Similarly, the IS-only cohort showed an early and rapid rise in CSF GalCer 18:0 (Figure 3B). Normal values are represented by gray shading (<10 ng/mL). As seen with psychosine concentration, in the 2Wk-High and 2Wk-Low cohorts CSF GalCer 18:0 was significantly reduced in comparison with IS-only dogs at 8 (P = 0.0047, P = 0.0209) and 12 (P = 0.0047, P = 0.0209) weeks of age, respectively. CSF GalCer in the 2Wk-High cohort was significantly different from normal from 36 to 48 weeks of age (P = 0.0201); however, it was not significantly different before 36 weeks or at 1 year of age (P = 0.1213) (Supplemental Table 1).

Similarly to CSF psychosine and GalCer, CSF total protein increased with disease progression in untreated GLD dogs (Sup-

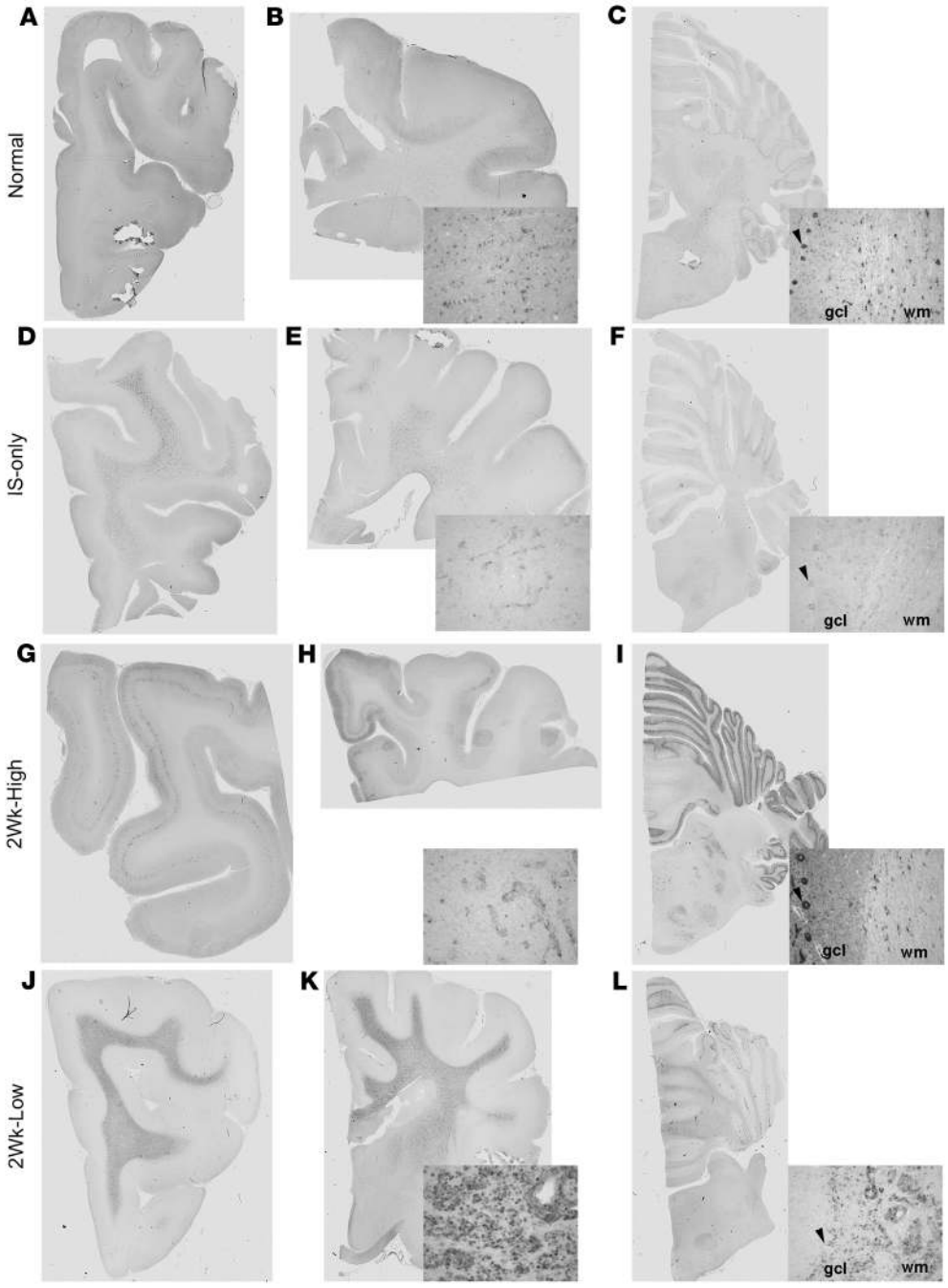

Figure 5. GALC immunohistochemical staining of the brain. IHC staining with GALC antibody of the frontal lobe, corona radiata/internal capsule, and cerebellum in normal dog (**A**–**C**), IS-only dog (**D**–**F**), 2Wk-High dog (**G**–**I**), and 2Wk-Low dog (**J**–**L**). Insets show higher-magnification images of whole-slide scans. Black arrowheads indicate Purkinje cells. gcl, granule cell layer; wm, white matter.

plemental Figure 2). In contrast, the 2Wk-High cohort showed normal CSF protein (≤30 mg/dL) throughout the entire period of observation. The 2Wk-Low and 6Wk-High cohorts showed CSF protein concentrations that increased with age and exceeded normal concentrations by 28 weeks of age, and the 6Wk-Low cohort exhibited a more rapid increase in CSF protein that exceeded normal levels by 16 weeks of age (Supplemental Figure 2). Thus, like CSF psychosine and GalCer, total CSF protein is associated with disease severity and therapeutic efficacy.

Peripheral nerve conduction velocities and auditory central conduction times are improved in GLD dogs treated presymptomatically with 1 × 10^{14} vg AAV9-cGALC. Motor (tibial, ulnar) and sensory (radial) nerve conduction velocities are significantly reduced in untreated GLD dogs as compared with normal age-matched control dogs, with the degree of velocity reduction consistent with demyelination (12, 17). IS-only GLD dogs were not significantly different from untreated GLD dogs in the 3 nerves analyzed at 8 weeks of age (Figure 4A). At 16 weeks of age, the 2Wk-High, 2Wk-Low, and 6Wk-High cohorts had nerve conduction velocities not significantly different from normal for each of the 3 nerves analyzed ($P > 0.05$) (Figure 4B). At 24 weeks of age, the 2Wk-High and 2Wk-Low cohorts remained not significantly different from normal, while the 6Wk-High cohort showed significantly reduced velocities for the tibial ($P = 0.0201$), ulnar ($P = 0.0201$), and radial ($P = 0.0389$) nerves (Figure 4C). At 52 weeks of age, the 2Wk-High cohort remained not significantly different from normal for the tibial and radial nerves ($P > 0.05$), but showed reduced velocities in the ulnar nerve ($P = 0.019$) (Figure 4D). The 6Wk-Low cohort had significantly slower nerve conduction velocity in ulnar ($P = 0.008$) and radial ($P = 0.0079$) nerves at 8 weeks of age. As only 2 dogs in this cohort lived to 16 weeks of age, statistics could not be done. Together, these results reveal that intracisternal delivery of AAV9-cGALC was capable of correcting nerve conduction velocity associated with demyelination when performed presymptomatically, while the postsymptomatic effect was transient.

Brainstem auditory evoked response testing showed that wave forms were degraded and central conduction times (I-V peak latency of waves) were significantly increased in untreated GLD dogs at 16 weeks of age as compared with normal age-matched controls (left ear, $P = 0.0105$; right ear, $P = 0.0196$) (Supplemental Figure 3 and Supplemental Table 1). At 16 weeks of age, the 2Wk-High cohort exhibited normalized central conduction times (left ear,

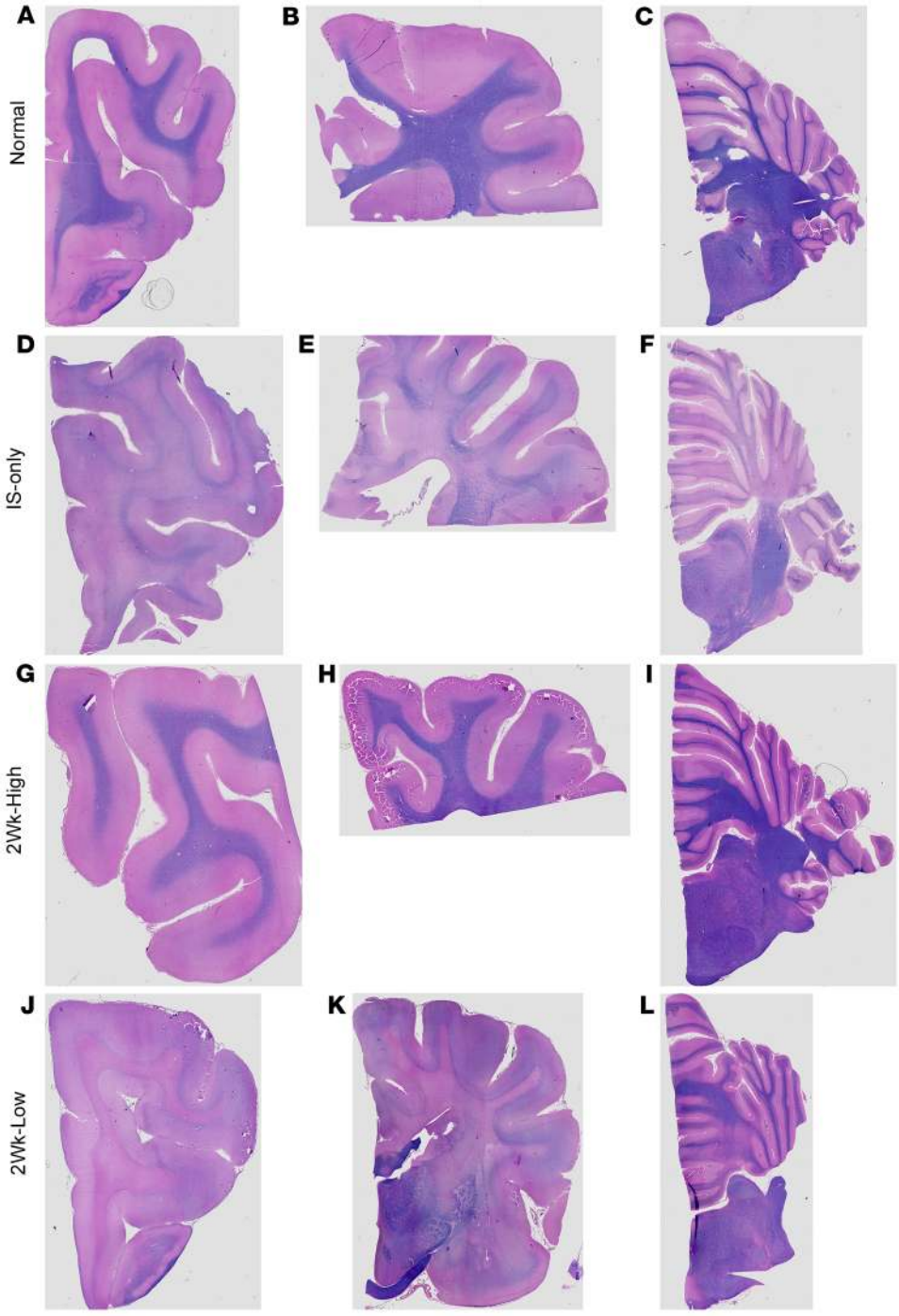

Figure 6. Iron eriochrome staining of the brain. Iron eriochrome staining of myelin in normal dog (**A**–**C**), IS-only dog (**D**–**F**), 2Wk-High dog (**G**–**I**), and 2Wk-Low dog (**J**–**L**).

$P = 0.4762$; right ear, $P = 0.3275$) that were significantly improved in comparison with untreated GLD dogs (left ear, $P = 0.0066$; right ear, $P = 0.0132$). Similarly, the 2Wk-Low cohort had conduction times that were not significantly different from normal (left ear, $P = 0.5169$; right ear, $P = 0.169$) and were significantly reduced in comparison with untreated GLD (left ear, $P = 0.0339$; right ear, $P = 0.0253$). The 6Wk-High cohort had central conduction times not significantly different from those in normal or untreated GLD ($P > 0.05$), suggesting an intermediate correction. The 6Wk-Low and IS-only cohorts had 2 dogs alive at 16 weeks of age, so statistics could not be done; however, conduction times remained increased (Supplemental Figure 3). At 52 weeks of age the 2Wk-High cohort remained not significantly different from normal (left ear, $P = 0.4472$; right ear, $P = 0.8057$). Together, these results reveal that intracisternal delivery of AAV9-cGALC was capable of normalizing central conduction time when performed presymptomatically.

Global expression of GALC and attenuation of both CNS and PNS pathology in dogs treated presymptomatically with 1×10^{14} vg AAV9-cGALC. Immunohistochemical (IHC) staining with an antibody specific to GALC revealed GALC expression at low levels in glial cells of the white matter throughout the brain of normal dogs (Figure 5, A–C). GALC expression was not detectable in cortical neurons (Figure 5A) but was present in Purkinje cells (Figure 5C, inset, arrowhead). In untreated and IS-only dogs (Figure 5, D–F), GALC was present throughout the white matter in dense regions of globoid cell accumulation. GALC expression was not seen in cortical neurons (Figure 5D) and was just at the level of detection in Purkinje cells (Figure 5F, inset, arrowhead). In contrast to all other cohorts, in 16-week-old dogs in the 2Wk-High cohort, strong GALC expression in the majority of neurons of cortical layer V was detected (Figure 5G). GALC expression was present in both glia throughout the white matter and limited globoid cells isolated to the centrum semiovale (Figure 5H and Supplemental Table 1, Globoid Cells). In the cerebellum there was robust expression of GALC in nearly every Purkinje cell to a greater degree than in normal dogs and strong positive expression in glial cells in cerebellar white matter (Figure 5I, and inset). Cells in the white matter are presumed to be oligodendrocytes based on morphology (Figure 5I, inset, wm); however, colabeling with GALC and oligodendrocytes was not feasible because of antibody incompatibility in canine tissues. In the 2Wk-Low cohort at endpoint, GALC expression was seen throughout the white matter in dense regions of globoid cell accumulation (Figure 5, J–L). GALC

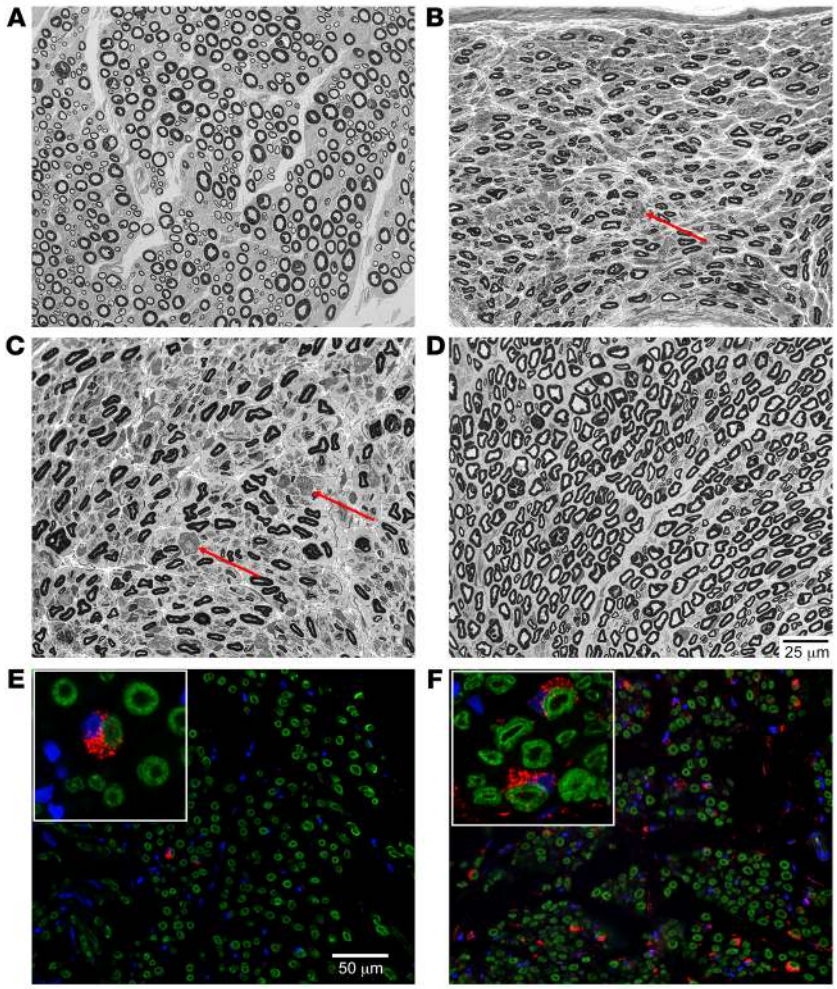

Figure 7. Light-level 1-μm resin sections and GALC immunofluorescence of tibial nerve. Resin-embedded samples from the tibial nerve were stained with paraphenylenediamine, then evaluated in 1-μm sections. (**A**) Normal dog 16 weeks of age. (**B**) IS-only 13 weeks of age. (**C**) 2Wk-Low 29 weeks of age. (**D**) 2Wk-High 16 weeks of age. (**E** and **F**) Immunofluorescent staining for GALC in red and myelin basic protein in green at ×40 original magnification in 2Wk-Low (**E**) and 2Wk-High (**F**) cohorts. Arrows in **B** and **C** point to myelin ovoids. Insets show Schwann cells at high magnification (×100). Scale bars: 25 μm, **A**–**D**; 50 μm, **E** and **F**.

was absent in the cerebral cortex and present in superficial Purkinje cells, but absent in deeper regions of the folia.

The 2Wk-High cohort dog with the lowest level of GALC enzyme activity in the internal capsule and cerebellum by enzyme assay is represented in Figure 5 to ensure no overrepresentation. GALC IHC in additional normal, IS-only, 2Wk-High, and 2Wk-Low dogs can be seen in Supplemental Figure 4. A similar pattern of expression was present in all dogs. Supplemental Figure 4 represents the 2Wk-High dog with the highest level of GALC enzyme activity in the cerebellum by enzyme assay so that the spectrum of expression can be appreciated. GALC expression from a third dog from the 2Wk-High cohort can be seen in the graphical abstract.

Globoid cell accumulation is the hallmark pathology in GLD and was evaluated in all cohorts by semiquantitation of H&E stain (Supplemental Table 1, Globoid Cell Accumulation). The IS-only cohort was indistinguishable from untreated GLD dogs, with marked, widespread globoid cell accumulation in the white matter. In contrast, in the 2Wk-High cohort, throughout the entire brain the only presence of globoid cells was in the centrum semiovale, the origin of pathology in Krabbe disease, and the corona radiata in 1 of 4 dogs (Supplemental Table 1). The globoid cell presence was less severe than in the IS-only and 2Wk-Low cohorts. In the 2Wk-Low cohort, globoid cell accumulation was more severe than in the IS-only cohort, likely owing to the advanced age of the dogs. Generally, there was a lessening of globoid cell infiltration in the cerebellum, nearest the injection site, and spinal cord in the 2Wk-Low cohort (Supplemental Table 1).

Both untreated and IS-only–treated GLD dogs had marked loss of myelin throughout the brain as visualized and semiquantified by iron eriochrome stain (Figure 6 and Supplemental Table 1, Demyelination). In the 2Wk-High cohort, as with globoid cell accumulation, demyelination was isolated to the centrum semiovale and corona radiata, which corroborates MRI signal intensity findings. In the 2Wk-Low cohort at humane endpoint, myelination was nearly absent in the most rostral brain as well as the centrum semiovale, corpus callosum, and internal capsule, exceeding severity of the IS-only cohort, likely owing to the advanced age (Figure 6K and Supplemental Table 1). Myelin was more preserved in the cerebellar folia but was diminished in the deep cerebellar white matter. These findings corroborate MRI findings in which the 2Wk-Low cohort had preservation in the cerebellum but not more rostral brain regions.

We next evaluated regions where gadolinium enhancement and presumed blood-brain barrier disruption were detected on MRI. Histology showed perivascular cuffing and infiltration of lymphocytes (Supplemental Figure 1G) in these regions, in addition to both severe demyelination (Supplemental Figure 1H) and infiltration of periodic acid–Schiff–positive storage granules (Supplemental Figure 1I).

In the PNS, GALC enzyme expression was present in numerous Schwann cells (>12 in a ×40 field; Figure 7F) of the tibial nerves of dogs in the 2Wk-High cohort. In the 2Wk-Low cohort, substantially fewer GALC-expressing Schwann cells were seen (2 in a ×40 field; Figure 7E). There also appears to be a subjective increase in the expression of myelin basic protein staining in the 2Wk-High cohort as compared with the 2Wk-Low cohort (Figure 7, E and F). Representative paraphenylenediamine-stained resin sections (1 μm) are shown of the tibial nerve. Compared with IS only, there was a subjective increase in the population of small- and large-caliber nerve fibers in both AAV-treated cohorts. Active axonal degeneration (swollen axons, accumulation of degenerating organelles)

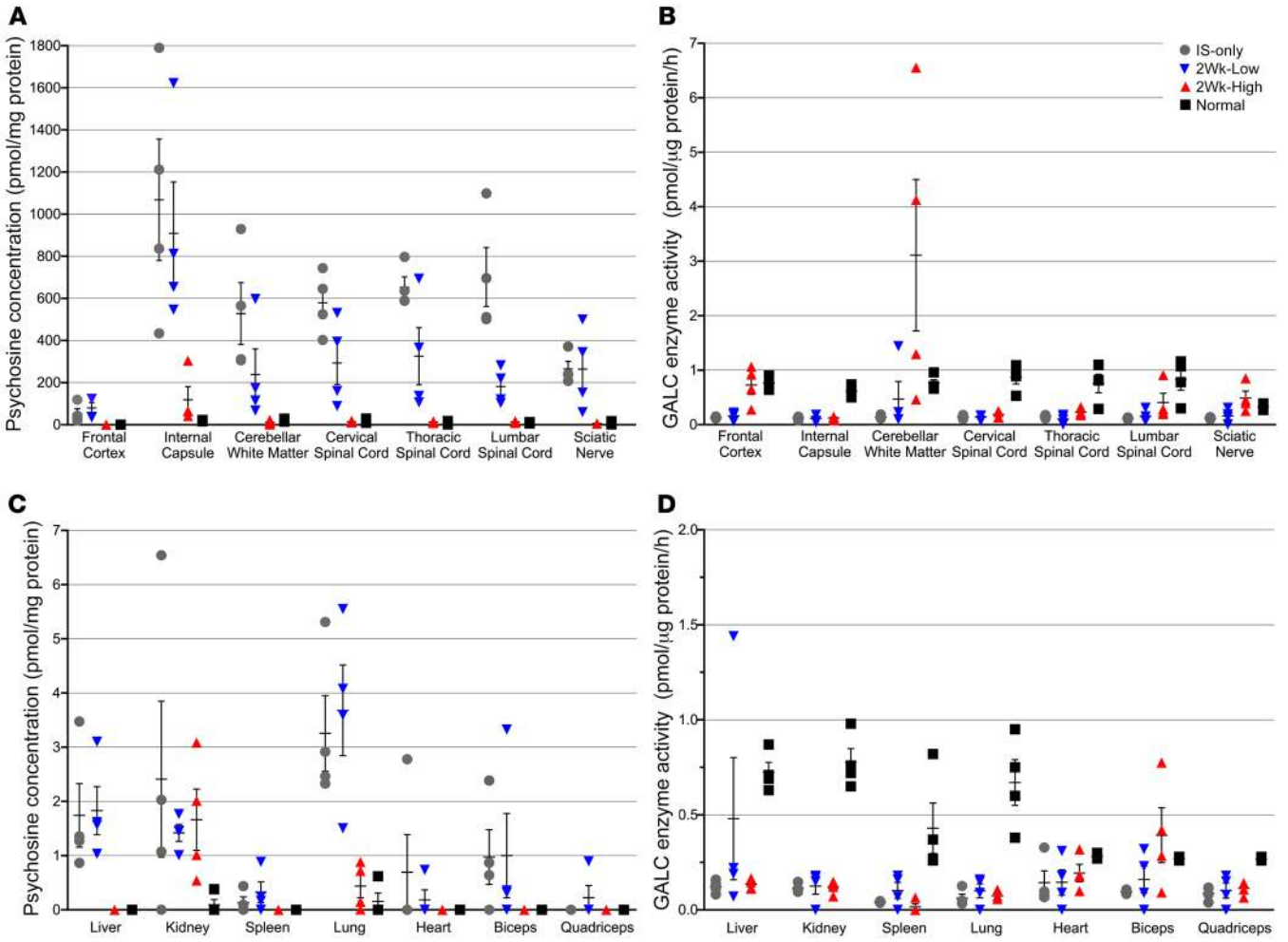

Figure 8. Psychosine concentration and GALC enzyme activity. Psychosine concentration was determined by mass spectrometry and GALC enzyme activity was measured using a synthetic 4MU substrate in punch biopsies taken from flash-frozen tissue samples of the frontal cortex, internal capsule, cerebellar white matter, cervical spinal cord, thoracic spinal cord, lumbar spinal cord, sciatic nerve, liver, kidney, spleen, lung, heart, biceps, and quadriceps. Psychosine (**A** and **C**) is reported in pmol/mg protein and GALC enzyme activity (**B** and **D**) in pmol/μg protein per hour. IS-only cohort at endpoint (n = 4, gray circles), 2Wk-High cohort at 16 weeks of age (n = 4, red triangles), 2Wk-Low cohort at endpoint (n = 4, blue triangles), normal at 16 weeks of age (n = 4, black squares). Lines represent mean with SEM. Nonparametric Kruskal-Wallis test and Mann-Whitney test were performed. A P value of less than 0.05 was considered significant.

was not observed in any cohort; however, rare myelin ovoids consistent with end-stage axonal degeneration were found in the IS-only (Figure 7B, arrow) and 2WK-Low GLD (Figure 7C, arrows) cohorts. Myelin ovoids were not found in the 2WK-High GLD (Figure 7D) cohort. Myelinated fiber density (MFD; myelinated fibers/mm^2) of the tibial nerve of normal 16-week-old dogs was determined to be 9891.5 ± 1704.7 and the percentage of thinly myelinated fibers (<5 μm) 23.8% ± 3.1% (n = 4) (Figure 7A). Untreated GLD dogs had a reduction in MFD to 7764 ± 1734 and an increase in the percentage of thinly myelinated fibers to 31.4% ± 7.1% (n = 4). In the 2Wk-Low dose cohort, data were available from 2 dogs with MFD of 9940 and 5544 and percentage of thinly myelinated fibers 23.7% and 15.2%, respectively (Figure 7C). The 2Wk-High dose cohort showed improvement over untreated GLD dogs with MFD in 2 dogs with data available at 7632 and 11,025 and percentage of thinly myelinated fibers 27.1% and 26.1%, respectively (Figure 7D). Together, our results indicate that after a single intracisternal injection of high-dose AAV9-cGALC, GALC expression is evident in Schwann cells and myelination is clearly improved.

Finally, given recent concern regarding toxicity to the dorsal root ganglia associated with AAV administration, we examined dorsal root ganglia as well as spinal cord gray matter. Within these regions we identified neuronal cytoplasmic swelling and Nissl substance loss (Supplemental Figure 5, red arrow) and, less frequently, cytoplasmic vacuolation (Supplemental Figure 5B, black arrow) with occasional accumulation of brightly eosinophilic granules (Supplemental Figure 5, blue arrows) and adjacent axonal swelling. These changes are unusual and may represent a secondary lesion due to chronic neuronal degeneration or axonal damage. This change is seen in most animals and is therefore likely unrelated to the treatment. A few animals also had minimal multifocal increased cellularity in the dorsal root ganglia, which may represent inflammatory cell infiltrates (Supplemental Figure 5C, green arrow); however, this was present across cohorts and thus is likely unrelated to treatment.

Psychosine, GALC enzyme activity, and vector copy quantification in AAV9-GALC–treated dogs. Remarkably, in the 2Wk-High cohort at 16 weeks of age, psychosine concentration was significantly reduced in comparison with IS-only dogs in all CNS tissues analyzed (frontal cortex, $P = 0.02$; internal capsule, $P = 0.02$; cerebellar white matter, $P = 0.02$; cervical spinal cord, $P = 0.02$; thoracic spinal cord, $P = 0.02$; lumbar spinal cord, $P = 0.02$) as well as in the sciatic nerve ($P = 0.02$) (Figure 8A). The internal capsule remained significantly higher than normal ($P = 0.02$); however, no other CNS or PNS tissues had psychosine values significantly different from those in normal age-matched control dogs ($P > 0.05$). Interestingly, in the cerebellar white matter and sciatic nerve, where GALC enzyme activity exceeded normal (Figure 8B), psychosine levels were 1.9- and 1.3-fold lower than normal, respectively. In the 2Wk-Low cohort, significant reduction of psychosine was seen only in the lumbar spinal cord ($P = 0.02$) (Figure 8A). Further, all nervous system tissue had psychosine values that remained significantly higher than in normal age-matched control dogs and the 2Wk-High cohort ($P < 0.05$).

In somatic tissues, the 2Wk-High cohort's lung psychosine levels were significantly reduced as compared with those of IS-only dogs ($P = 0.02$) and not significantly different from those of normal age-matched control dogs ($P > 0.05$) (Figure 8C). In the kidney, the psychosine concentration was not significantly different from that in the IS-only or the normal cohort. Numerous tissues from the 2Wk-High cohort had psychosine concentrations below the level of detection (liver, spleen, heart, biceps, and quadriceps). In contrast, the 2Wk-Low cohort had detectable levels of psychosine that were not significantly reduced as compared with IS-only–treated dogs in every somatic tissue sampled (Figure 8C). Additionally, liver, lung, and biceps psychosine levels remained significantly higher than in normal age-matched control and 2Wk-High cohorts ($P < 0.05$).

In the 2Wk-High cohort, GALC enzyme activity was significantly increased in comparison with the IS-only–treated cohort in all CNS (frontal cortex, $P = 0.02$; cerebellar white matter, $P = 0.02$; thoracic spinal cord, $P = 0.04$; lumbar spinal cord, $P = 0.02$) and PNS (sciatic nerve, $P = 0.02$) tissues analyzed except the internal capsule and cervical spinal cord ($P > 0.05$) (Figure 8B). Most notably, GALC enzyme activity was 4-fold higher than normal in the cerebellum, the area closest to the injection site, and 1.5-fold higher than normal in the sciatic nerve (Figure 8B). This corroborates our findings of GALC enzyme expression by IHC and immunofluorescence (Figures 5 and 7). In the 2Wk-Low cohort at endpoint, GALC was not significantly increased in comparison with the IS-only cohort in any CNS or PNS tissue ($P < 0.05$). GALC levels were not significantly different from normal ($P > 0.05$) in the cerebellar white matter or sciatic nerve, suggesting an intermediate level of restoration in those 2 tissues. There was no significant difference between the 2Wk-High and 2Wk-Low cohorts in somatic tissues ($P > 0.05$) (Figure 8D). A single intrathecal injection of high-dose, but not low-dose, AAV9-cGALC was able to significantly increase GALC enzyme activity and reduce psychosine concentration in CNS, PNS, and somatic tissues.

To evaluate AAV9 biodistribution after intracisternal delivery, we quantified vector genome (vg) copies per diploid genome in untreated, 2Wk-High, and 2Wk-Low GLD dogs. In alignment with the psychosine and GALC data, vg copies were significantly increased in the 2Wk-High cohort as compared with untreated dogs in all CNS tissues (frontal cortex, $P = 0.02$; cerebellar white matter, $P = 0.02$; cervical spinal cord, $P = 0.02$; thoracic spinal cord, $P = 0.02$; and lumbar spinal cord, $P = 0.02$) except the internal capsule. The 2Wk-Low cohort had significantly increased vg copies as compared with untreated animals in the frontal cortex ($P = 0.03$) and thoracic ($P = 0.03$) and lumbar ($P = 0.03$) spinal cord. However, all CNS tissues had significantly fewer vg copies than the 2Wk-High cohort ($P < 0.05$) except the internal capsule (Supplemental Table 1, Vector Genome Copies). The sciatic nerve was not analyzed for vg copies because of the limited amount of tissue for biochemistry (GALC and psychosine) and histology. In somatic tissues, the 2Wk-High cohort had a significant increase in vg copies as compared with untreated animals in all tissues except the quadriceps. The 2Wk-Low cohort had significantly more vg copies than untreated animals only in the liver ($P = 0.03$) and kidney ($P = 0.03$), and had significantly fewer vgs than the 2Wk-High cohort in all tissues except the quadriceps (Supplemental Table 1, Vector Genome Copies). Our results indicate that an intracisternal injection of AAV9 is capable of disseminating therapeutic transgenes throughout the CNS and somatic tissues, with the greatest number of vg copies in the spinal cord and liver, and with copies persisting for at least 16 weeks. These studies in a large-animal model provide strong evidence that a single injection of AAV9 into the CSF is capable of distributing functional therapeutic enzyme to the CNS, PNS, and somatic tissues where long-term expression prevents substrate accumulation, preserves myelin integrity, and prevents disease progression in a clearly dose-dependent manner.

Discussion

In GLD, both CNS and PNS myelination abnormalities occur, resulting in cognitive decline and motor deterioration that ultimately results in early death. Newborn screening for Krabbe disease is currently performed in many states, allowing for treatment of presymptomatic babies with HSCT. The exact therapeutic mechanism of HSCT is unknown; however, it is believed to involve transit of GALC-positive donor-derived monocytes into the CNS, which allows secretion of GALC to be endocytosed by neurons and glia via the mannose-6-phosphate receptor to cross-correct the enzyme deficiency (18). There are also data showing that HSCT has a significant immunomodulatory effect (19). Although HSCT is the standard of care for presymptomatic Krabbe infants, the majority of treated patients show limited improvements in motor ability and PNS myelination (5–9). Treated children are frequently wheelchair bound, unable to communicate effectively, and respirator dependent for an extended time. As HSCT in postsymptomatic children provides no increase in survival (6), it is no longer indicated for babies diagnosed beyond a couple of months of age. Clearly, there is a need for more effective therapies that treat both CNS and PNS aspects of disease at both presymptomatic and postsymptomatic stages.

Intrathecal administration of AAV9 permits dissemination of transgenes throughout the nervous system and is currently in clinical trials for the treatment of neuronal ceroid lipofuscinosis 3 (CLN3; ClinicalTrials.gov NCT03770572), CLN6 (NCT02725580), spinal muscular atrophy (NCT03381729), and

giant axonal neuropathy (NCT02362438). Because of its ability to cross the blood-brain barrier, AAV9 can be delivered intravenously to treat the CNS. However, intrathecal administration has many advantages, including higher transduction efficiency of the CNS (20); sustained expression with the absence of toxicity (21) seen with systemic delivery (22); evasion of anti-AAV neutralizing antibodies (23), which have been shown to be detrimental to systemic delivery (24); and requirement of substantially less vector product, increasing the feasibility of translation to human patients. Intrathecal AAV9-mediated gene therapy for Krabbe disease was first evaluated in the twitcher mouse (25, 26). When postnatal day 10–11 twitcher mice received a single lumbar intrathecal injection at a dose of 2×10^{11} vg, survival was modestly extended by about 10.5 days. This treatment improved the pathology and reduced psychosine levels but did not restore them to baseline levels (15). Notably, at postnatal day 10–11, twitcher mice are postsymptomatic, with reduced body weight and disease pathology present. Presymptomatic intrathecal injections were not performed, presumably because of the small size of the newborn mouse and the compressed timeline of disease progression.

In the GLD dog, we evaluated the efficacy of intrathecal administration of AAV9-cGALC in both presymptomatic and symptomatic dogs. Vector was administered at the cisterna magna, since we and others have shown that intracisternal AAV9 administration is safe in cats, dogs, and nonhuman primates and results in up to 100-fold more efficient gene transfer to the brain than does administration via lumbar puncture (27) or intravenously (20). Intracisternal AAV9 is currently being administered to patients with mucopolysaccharidosis I (NCT02362438) and GM1 gangliosidosis (NCT04273269) in clinical trials, making this a clinically relevant route of administration. Herein we have established that presymptomatic administration of high-dose (1×10^{14} vg) AAV9-cGALC into the CSF of GLD dogs ameliorates disease beyond 2.5 years of age, with all dogs in the 2Wk-High cohort currently alive and neurologically normal between 92 and 136 weeks of age (117.2 ± 18.0, $n = 6$), more than 7 times longer than untreated GLD dogs. These dogs continue to be monitored by neurological examination, MRI, nerve conduction velocity testing, and brainstem auditory evoked response. Serum and CSF samples are routinely collected for additional long-term analyses.

The results in the dog far exceed expectations based on the findings in the twitcher mouse. The intrathecal dose of 2×10^{11} vg in the twitcher mouse is roughly equivalent to the low dose administered to GLD dogs if scaled by brain weight or CSF volume. Indeed, we saw a clear dose response to AAV9-cGALC in the GLD dogs. Reduction of the dose to 2×10^{13} vg resulted in doubling of lifespan in the GLD dog (untreated GLD dogs, 15.7 ± 4.8 weeks of age [ref. 12]; 2Wk-Low, 30.43 ± 2.65 weeks of age). Postsymptomatic administration of 2×10^{13} vg to dogs (6Wk-Low), the experimental protocol most similar to the twitcher mice, did not significantly increase survival time in comparison with untreated GLD dogs. Additionally, the twitcher mouse results from a nonsense mutation (c.339G>A) and makes no functional GALC protein (26). Twitcher mice dosed intrathecally with AAV9-mGALC did not receive immunosuppression (15) and thus may have developed an immune response that diminished transgenic protein expression. In fact, CNS-directed AAV-mediated gene therapy has previously been shown to elicit an immune reaction even in newborn twitcher mice (19). In contrast, GLD in the dog results from a missense mutation (c.473A>C; p.158Y>S) (10) with low levels of GALC enzyme detectable in the CNS, PNS, and somatic tissues (ref. 17 and Figure 7). In addition to this immunological advantage, GLD dogs received high-dose immunosuppression before gene transfer and maintenance immunosuppression for 4 months, preventing immune-driven decreases in transgenic protein expression. Thus, the canine model will likely express greater levels of both endogenous and transgenic GALC following AAV9-GALC therapy than will twitcher mice.

Importantly, presymptomatic dogs that received 2×10^{13} vg exhibited incomplete disease correction and the emergence of clinical signs not typically seen in untreated GLD dogs, which reach humane endpoint (pelvic limb paralysis) at a significantly younger age (12). The delayed progression of motor deficits seen in these dogs correlates with normalization of cerebellar white matter signal intensity and cerebellar area on MRI. While cerebellar disease was ameliorated, pathological signs emerging in 2Wk-Low–treated dogs included behavioral abnormalities and visual deficits. Blindness is likely central in origin as no retinal abnormalities were observed and demyelination and perivascular cuffing were observed in the occipital lobes. Fascinatingly, these clinical findings are similar to those in late-infantile-onset and juvenile-onset patients, who all fall below the 5th percentile in cognitive development by 40 months of age, with vision deterioration observed in the majority (3). These data suggest that treatment with an inadequate dose of AAV9-cGALC provides insufficient GALC enzyme resulting in an attenuated form of the disease with substantial impairments.

Additionally, the canine model of GLD allowed for comparison of pre- and postsymptomatic gene delivery. Our studies found that postsymptomatic therapy was less effective than presymptomatic therapy at the respective doses evaluated. Remarkably, however, dogs treated with 1×10^{14} vg postsymptomatically showed slowing of clinical disease progression, significantly prolonged survival, and reduced CSF protein levels. This outcome stands in stark contrast to HSCT, which is only effective presymptomatically (6). We speculate that postsymptomatically treated dogs did not fare as well as those treated presymptomatically because of reduced vg dose relative to their larger brain and body size at the time of treatment. Two-week-old normal dogs from this specific breeding line have an average brain weight of 26.06 ± 2.23 g ($n = 10$), while analogous 6-week-old dogs have an average brain weight of 52.91 ± 5.56 g ($n = 10$). Based on this, the dogs in the 2Wk-High cohort received an estimated 3.84×10^{12} vg/g of brain weight while dogs in the 6Wk-High cohort received an estimated 1.89×10^{12} vg/g of brain weight, essentially reducing the normalized dose by half. Notably, the single remaining dog in the 6Wk-High cohort, currently 97.1 weeks of age, was the smallest dog within that cohort at the time of treatment, effectively giving the dog a larger dose per gram of body weight and brain weight. While systemic delivery of AAV is conventionally normalized to body weight, our data suggest that intrathecal delivery of AAV would also benefit from normalization to body weight, estimated brain weight, or CSF volume. As such, we predict that normalization of dosing is likely to further improve prognosis for dogs treated postsymptomatically.

Krabbe disease in patients results from more than 200 pathogenic variants. In patients of northern European decent, a 30-kb deletion and 2 missense mutations, c.1586C>T; p.T529M and c.1700A>C; p.Y567S, are expected to account for 50% to 60% of pathogenic alleles in the infantile onset (28, 29). While the naturally occurring canine model has genetic limitations, the missense mutation may be representative of a large population of Krabbe disease patients and how they would respond to gene therapy. Since we were able to establish a robust, clinically relevant biomarker in the canine model, this could potentially be useful to normalize therapeutic responses among different mutations. In Krabbe disease patients, psychosine is a diagnostic marker of phenotype severity and treatment effect (30, 31). Similarly, we have shown that CSF psychosine increased early and steadily in untreated GLD and strongly correlated with disease progression (16). In the 2Wk-Low cohort, detection of psychosine in the CSF was delayed until 12 weeks of age. In the 2Wk-High cohort, CSF psychosine remained undetectable up to 24 weeks, and from 24 to 52 weeks psychosine was detected in the CSF of only 1 dog, which currently remains asymptomatic. If psychosine is indeed a robust biomarker of therapeutic outcome, we predict that this one dog will eventually fare less well than other dogs in the cohort.

CSF protein concentration has recently been shown to predict age of disease onset and survival in a study of 248 Krabbe disease patients (4). Comparably, we show that CSF protein increases early and steadily, with levels rising above normal in untreated GLD dogs by 8 weeks of age. Notably, CSF protein concentration in the 2Wk-High cohort remains within normal levels beyond 52 weeks of age, consistent with their increased longevity and reduced pathology. In contrast, the 2Wk-Low and 6Wk-High cohorts reached above normal CSF protein levels, and the 6Wk-Low cohort emulated untreated GLD dogs with an early, rapid increase in CSF protein. The single 2Wk-High cohort dog with elevated psychosine also has the highest CSF protein, 21 mg/dL at 1 year of age, although still within normal limits.

Postmortem evaluation of the 2Wk-High cohort at 16 weeks of age demonstrated global transduction of the CNS with a significant increase in GALC enzyme activity and significant reduction in psychosine concentration in the most rostral brain region sampled, the frontal cortex. GALC enzyme activity levels approximately 4 times normal were seen in the cerebellar white matter, the tissue sampled closest to the injection site. Interestingly, psychosine concentration was below normal levels in this brain region. Despite attainment of supraphysiological levels of a normally low-expressing enzyme, no evidence of toxicity was noted in any dog, and no lesions were noted on MRI or on histological evaluation near the injection site. MRI lesions have previously been demonstrated in nonhuman primates, in which toxicity due to overexpression of a different secreted hydrolytic lysosomal enzyme occurred (32).

Variability in tissue psychosine concentrations and GALC activity was minimal within the 2Wk-High cohort, all sacrificed at 16 weeks of age, signifying reproducibility of this treatment approach. In contrast, variability was seen within the IS-only and 2Wk-Low cohorts, which were followed until humane endpoint. We recently reported that CSF psychosine concentrations vary and closely correlate with disease progression in GLD dogs (16), and this is likely true for tissues. Interestingly, the youngest dog to develop pelvic limb paralysis in the IS-only cohort had the highest psychosine levels in the sciatic nerve (Dog 1, Supplemental Table 1). Similarly, in the 2Wk-Low cohort, the single dog that reached humane endpoint solely due to pelvic limb paralysis and not combinatorial factors of blindness and behavior concerns had the highest psychosine concentration in the sciatic nerve (Dog 16, Supplemental Table 1). It is hypothesized that assessment of psychosine concentrations following biopsy of peripheral nerves in patients may yield important information regarding clinical outcome.

Psychosine concentrations were highest in all cohorts in the internal capsule. The internal capsule was the single nervous system tissue in which presymptomatic high-dose AAV did not normalize psychosine and GALC and did not achieve a significant increase in vg copies. It is probable that psychosine had already accumulated to irreversible levels by the time of treatment at 2 weeks of age or, alternatively, cell death and globoid cell formation in this area did not allow for sufficient transduction of therapeutic GALC. Ongoing studies using MALDI mass spectrometry will help elucidate the temporospatial accumulation of psychosine in canine GLD. It has recently been shown in the twitcher mouse that inhibitory effects of psychosine are visible as early as embryonic day 12 (33). Taken together, these findings reiterate the importance of early intervention.

Biochemical findings were corroborated by MRI and histology. In the 2Wk-High cohort, T2-weighted hyperintensity was most apparent on MRI at the centrum semiovale, a region for pathology initiation in Krabbe disease (34, 35). Notably, the lesion was stable from 16 to 52 weeks, suggesting that pathology was likely present at the time of treatment and did not progress thereafter. Histology confirmed this to be a region of demyelination, necrosis, and globoid cell accumulation.

Histological evaluation of GALC by IHC revealed that in untreated and IS-only GLD dogs GALC was detectable in globoid cells densely accumulated in the white matter. The same distribution was seen in the 2Wk-Low cohort, but in greater intensity likely due to the prolonged age. The 2Wk-High cohort demonstrated cortical neurons and Purkinje cells strongly expressing GALC to a greater degree than normal age-matched controls, suggesting either the transduction of these cells or the accumulation of GALC due to mannose-6-phosphate receptor–mediated endocytosis. Quantification of IHC-positive GALC cells was not informative or reliable. The ability of the enzyme to actively cleave a substrate as measured by enzyme assay is more revealing as to the effect of AAV-delivered GALC.

Despite being delivered into the CSF, AAV vector copies were detectable in all somatic tissues analyzed. Intrathecally delivered AAV vectors are redistributed from the subarachnoid space to systemic circulation likely via the arachnoid villi (20). However, recent identification of the glymphatic, or glia-associated lymphatic, system has provided more insight into additional mechanisms that may control AAV clearance. Dysregulation of membrane channels in aged and diseased mouse brains correlated with significantly increased retention of AAV vectors in the brain and reduced systemic leakage (36). This has yet to be investigated in Krabbe disease.

Although effective therapies for CNS disease are being developed, the current inability to treat peripheral neuropathies

continues to impact the prognosis for patients with many lysosomal storage diseases. While cognitive function is improved in infants with Krabbe disease who receive HSCT, motor deficits and peripheral nerve dysfunction often persist (6, 37, 38). Here, in the canine GLD model, early delivery of high-dose, but not low-dose, AAV9-cGALC resulted in a significant increase in GALC enzyme activity and significant reduction of psychosine to below normal levels in the sciatic nerve after intracisternal delivery. Levels of GALC in the 2Wk-High cohort are 3.5 times higher in the sciatic nerve than in the liver, suggesting that the correction to the PNS is not due to leakage of vector or GALC into the periphery. The increase in sciatic nerve GALC activity could be due either to transduction of the lower motor neuron or dorsal root ganglia, resulting in increased axonal GALC, or to transduction of Schwann cells. The delivery of lysosomal enzymes to Schwann cells and axons of peripheral nerves has been previously described in dogs with mucopolysaccharidosis VII that received canine GUSB via intracisternally delivered AAV (39) and likely results from AAV passage down the nerves through endoneurial fluid (40–42) or axonal transport (43, 44). Importantly, in this study, nerve conduction velocity testing and PNS ultrastructure analysis show improved PNS myelination in treated dogs and corroborate the biochemical findings. Together, these findings provide what is to our knowledge the first demonstration of clinical, biochemical, and histological correction of PNS abnormalities in a large-animal model following intracisternal delivery of AAV9. This finding holds implications for treatment of other peripheral nerve disorders using this safe, effective, and proven route of administration.

We previously evaluated combination intravenous and intracerebroventricular administration of AAVrh10 in canine GLD (17). The studies cannot be directly compared because of different AAV serotypes, routes of administration, doses, and immunosuppression protocols. Nonetheless, intracisternal AAV9 evaluated herein resulted in what we believe to be the first extension of lifespan beyond 1 year of age in the GLD dog and more global correction of nervous system disease. Additionally, intracisternal delivery allowed for earlier intervention and required significantly less vector, permitting higher dosing and a more robust study design. Intracisternal AAV9 has shown unprecedented results in this large-animal model and is the most translatable approach evaluated to date. Long-term evaluation of the immune response to AAV9-cGALC, and its relation to circulating GALC enzyme activity, is ongoing and will be reported at the 2-year time point. Additionally, assessment of lumbar intrathecal delivery of AAV9-cGALC is under way and will help guide translation to the clinic.

Conclusions. In this robust study of 26 GLD dogs, we demonstrated that intracisternal delivery of 1×10^{14} vg AAV9-GALC into presymptomatic GLD dogs ameliorated neurological signs of disease beyond 2.5 years of age. Reducing the dose 5-fold resulted in significant extension of lifespan; however, an attenuated form of Krabbe disease developed, including behavioral abnormalities and blindness. Administration of 1×10^{14} vg at a symptomatic age, when HSCT no longer has clinical benefit, significantly extended lifespan and delayed disease progression, with 1 dog still alive beyond 1.5 years of age. Finally, in contrast to HSCT, which only treats CNS disease, intracisternal administration of AAV-GALC improved both CNS and PNS myelination. These results reiterate findings from other AAV9 clinical trials that high-dose and early intervention are necessary for AAV9 to provide the greatest benefit. In light of safety data of intrathecal delivery of AAV9 emerging from clinical trials for other diseases, we believe that this positive finding in a large-animal model of Krabbe disease warrants timely translation to the clinic.

Methods

Animals, immunosuppression, and AAV vector injections. Dogs were raised in the National Referral Center for Animal Models of Human Genetic Disease of the University of Pennsylvania School of Veterinary Medicine (NIH P40-OD-010939). GLD in dogs is due to a missense mutation in the *GALC* gene, c.473A>C; p.158Y>S. Whole blood from dogs was tested for the *GALC* mutation as previously described (12, 17).

One hour before intracisternal injection, methylprednisolone was delivered intravenously at a dose of 20 mg/kg. Immediately before intracisternal injection, the skin was clipped and scrubbed with 4% chlorohexidine followed by 70% isopropyl alcohol, and approximately 0.5 mL of CSF was collected from the cerebellomedullary cistern. Then 1.0 mL of AAV9-cGALC was delivered as a bolus over less than 1 minute. Dogs received oral prednisone at a dose of 0.5 mg/kg daily for 4 months followed by a 2-week taper. GLD dogs were euthanized using an overdose of intravenous barbiturate at a predetermined or standard humane endpoint. After sacrifice, animals were perfused through the left ventricle with 0.9% cold saline and tissues collected.

Vector production. AAV9-cGALC vector was produced with single-stranded AAV genome comprising an AAV2 inverted terminal repeat (ITR), the CAGGS version of the CBA promoter (1.6 kb total CMV enhancer, chicken β-actin promoter, and partial 5′-untranslated region), codon-optimized canine *GALC* DNA coding sequence (2055 bp), SV-40 polyadenylation signal (143 bp), and an AAV2 ITR. AAV vectors were produced at the University of North Carolina Vector Core as previously described (45). Purified AAV was dialyzed in PBS supplemented with 5% D-sorbitol and an additional 212 mM NaCl (350 mM NaCl total). Vector was titered by quantitative PCR (46), and confirmed by PAGE and silver stain.

Nerve conduction velocity, brainstem auditory evoked response, and MRI. Dogs were anesthetized with propofol, endotracheally intubated, and maintained on isoflurane anesthesia. Nerve conduction velocity was tested using an electrodiagnostics machine (Nicolet Viking Quest). Brainstem auditory evoked response data were recorded using a Nicolet Viking Quest machine (Nicolet Biomedical). Imaging was performed on anesthetized dogs on a 1.5-tesla MRI scanner (Signa, GE Corp.). Nerve conduction velocity testing, brainstem auditory evoked response recording, and MRI were performed as previously described (12, 13, 17).

Histology. Perfused brains were fixed in 4% paraformaldehyde and paraffin-embedded. Myelin staining and periodic acid–Schiff staining were performed as previously described (12, 17). For immunofluorescence, deparaffinized and rehydrated slides were heated to a boil followed by a 30-minute incubation in antigen retrieval solution (HK086, Biogenex). Primary rabbit polyclonal anti-GALC (AB137750, Abcam; 1:200) and rat monoclonal anti–myelin basic protein (NB600-717, Novus Biologics; 1:500) antibodies were diluted in antibody dilu-

ent solution (003118, Life Technologies) and incubated at 37°C for 1 hour. Following three 5-minute washes with PBS, donkey anti–rabbit IgG conjugated to Alexa Fluor 568 (A10042, Thermo Fisher Scientific) and donkey anti–rat IgG conjugated to Alexa Fluor 488 (A21208, Thermo Fisher Scientific) secondary antibodies were diluted 1:500 in antibody diluent solution and incubated at 37°C for 30 minutes. Following three 5-minute washes with PBS, slides were stained with DAPI for 1 minute and mounted. For IHC, following rehydration and antigen retrieval, slides were incubated in 3% hydrogen peroxide for 15 minutes to quench endogenous peroxidases and then rinsed. Sections were blocked for endogenous biotin with an avidin/biotin blocking kit (SP-2001, Vector Laboratories). GALC antibody was diluted and incubated as described for immunofluorescence, washed 3 times for 5 minutes in PBS, and incubated with a 1:500 dilution of biotinylated goat anti–rabbit IgG secondary antibody (BA-1000, Vector Laboratories) at 37°C for 30 minutes. Following three 5-minute PBS washes, sections were incubated with avidin–biotin–horseradish peroxidase complex (PK-6100, Vector Laboratories) at 37°C for 30 minutes. Following three 5-minute PBS washes, colorimetric signal was developed using a DAB kit (SK-4100, Vector Laboratories). Sections were dehydrated through ethanols, cleared in xylene, and mounted with Cytoseal XYL (8312-4, Thermo Fisher Scientific).

Detailed histological evaluation was performed in a blind fashion without knowledge of the experimental groups by a board-certified pathologist. Semiquantitative analysis of globoid cell accumulation, gliosis, and inflammation was performed on H&E sections, while the evaluation of demyelination was performed on adjacent sections stained with iron eriochrome stain.

Peripheral nerve analysis: light microscopy and morphometry. Peripheral nerve specimens were collected from the tibial nerves and prepared as previously described (12, 17). Qualitative morphometry was performed on nerve fibers adequately fixed and free of artifacts. Determinations included myelinated fiber density, split myelinated fiber density, thin myelinated fiber density, and cluster density.

Quantification of tissue GALC enzyme activity. Tissue homogenates (20 μg) in pure H_2O were incubated with fluorescent GALC substrate (6HMU-β-D-galactoside, Moscerdam Substrates) for 17 hours at 37°C. Enzymatic activity was assessed via fluorescence measured with a Beckmann Coulter DTX 880 multimode detector using excitation/emission wavelengths of 385 nm/450 nm.

Quantification of tissue psychosine. Psychosine from tissue homogenates (200 μg) was extracted via a methanol–acetic acid solution and analyzed as previously described (47). Analysis was then performed on a Shimadzu Nexera ultra-high-performance liquid chromatography system equipped with a Waters Acquity UPLC BEH amide column and coupled to a Shimadzu LCMS-8050 triple quadrupole mass spectrometer equipped with positive ion electrospray. D-Lactosyl-β1-1′-D-*erythro*-sphingosine (Avanti Polar Lipids) was used as an internal standard.

Quantification of CSF psychosine. CSF psychosine was determined as previously described (48). Protein precipitation was performed to extract psychosine from 50 μL of dog CSF. Deuterated galactosylsphingosine (psychosine-d_5; 1 ng/mL) was used as an internal standard. Sample analysis was performed with a Shimadzu 20AD HPLC system, coupled to a triple quadrupole mass spectrometer (API 4000 QTrap) operated in MRM mode. The positive ion ESI mode was used for detection of psychosine and psychosine-d_5. Data processing was conducted with Analyst 1.5.1 (Applied Biosystems).

Vector quantification. Vector biodistribution was done by quantitative PCR. Tissue DNA was purified and quantified as previously described (24) except that a QIACube HT system was used for genomic DNA purification. Quantification was directed to the codon-optimized canine *GALC* transgene, using primers that would not recognize the endogenous *GALC* gene. The primer sequences were as follows: cGALC-F-5′-GGCGTCCATGCTGCTTGATAG-3′; cGALC-R-5′-ACATCGCTGTTCAGGGTGGAG-3′; cSDHA-F-5′-GCGTTCCACTTGTCCCTGTA-3′; cSDHA-R-5-TCATCACTTCCCAACCTGGC-3′. Data are reported as the number of double-stranded *GALC* molecules per 2 double-stranded copies of the canine SDHA locus (the number of vector DNA copies per diploid canine genome).

Statistics. Data were evaluated for normal distribution by the skewness and kurtosis tests for normality, and the nonparametric Kruskal-Wallis test was used for the initial comparison of each variable between the different treatment groups. The Mann-Whitney test was performed for follow-up pairwise comparisons if the *P* value of the Kruskal-Wallis test was less than 0.05. A *P* value of less than 0.05 on the Mann-Whitney test, which does not assume that the variable is normally distributed, was considered significant. All statistical evaluations were performed using a statistical software package (Stata 14.0 for Macintosh, Stata Corp.).

Study approval. Dogs were raised in the National Referral Center for Animal Models of Human Genetic Disease of the University of Pennsylvania School of Veterinary Medicine (NIH P40-OD-010939) under NIH and US Department of Agriculture guidelines for the care and use of animals in research. The experimental protocol was approved by the University's Institutional Animal Care and Use Committee.

Author contributions

AMB, SJG, and CHV designed research studies. AMB, JHB, DN, EAL, JPS, XJ, GPS, IJH, KM, PO, and CHV conducted experiments. AMB, JHB, DN, EAL, JPS, XJ, AO, KM, DSO, CAA, GDS, ERB, SJG, and CHV acquired data. RSH, AMB, EAL, JPS, CAA, AO, GDS, and CHV analyzed data. MSS and SJG provided reagents. CAA analyzed histological sections. AMB, EAL, XJ, GPS, KM, MSS, CAA, DSO, GDS, ERB, SJG, and CHV wrote the manuscript.

Acknowledgments

We thank the veterinary technicians and students that cared for animals in these studies. We also thank Enrico Radaelli from the University of Pennsylvania Department of Pathology for his contribution to the histopathological evaluation. We acknowledge Violeta Zaric at the University of Texas Southwestern Viral Vector Facility for help with the quantitative PCR analysis. Our funding sources include NIH/NINDS-R01-NS096087 (to CHV), NIH-P40-OD010939 (to CHV), NIH/NINDS-F32-NS093898 (to AMB), NIH/NICHD-1K99-HD096115 (to AMB), and R01-NS065808 (to ERB).

Address correspondence to: Allison M. Bradbury, Abigail Wexner Research Institute, Center for Gene Therapy, Nationwide Children's Hospital, 700 N. Children's Drive, WA3016, Columbus, Ohio USA 43205. Phone: 614.355.2694; Email: Allison.Bradbury@nationwidechildrens.org.

AMB's present address is: Nationwide Children's Hospital, Abigail Wexner Research Institute, Center for Gene Therapy, Columbus, Ohio, USA.

1. Wenger DA, Escolar ML, Luzi P, Rafi MA. *Krabbe Disease (Globoid Cell Leukodystrophy)*. Columbus, Ohio, USA: McGraw-Hill; 2014.
2. Beltran-Quintero ML, et al. Early progression of Krabbe disease in patients with symptom onset between 0 and 5 months. *Orphanet J Rare Dis*. 2019;14(1):46.
3. Bascou N, DeRenzo A, Poe MD, Escolar ML. A prospective natural history study of Krabbe disease in a patient cohort with onset between 6 months and 3 years of life. *Orphanet J Rare Dis*. 2018;13(1):126.
4. Komatsuzaki S, et al. Clinical characteristics of 248 patients with Krabbe disease: quantitative natural history modeling based on published cases. *Genet Med*. 2019;21(10):2208–2215.
5. Wasserstein MP, et al. Clinical outcomes of children with abnormal newborn screening results for Krabbe disease in New York State. *Genet Med*. 2016;18(12):1235–1243.
6. Escolar ML, et al. Transplantation of umbilical-cord blood in babies with infantile Krabbe's disease. *N Engl J Med*. 2005;352(20):2069–2081.
7. Aldenhoven M, Kurtzberg J. Cord blood is the optimal graft source for the treatment of pediatric patients with lysosomal storage diseases: clinical outcomes and future directions. *Cytotherapy*. 2015;17(6):765–774.
8. Wright MD, Poe MD, DeRenzo A, Haldal S, Escolar ML. Developmental outcomes of cord blood transplantation for Krabbe disease: a 15-year study. *Neurology*. 2017;89(13):1365–1372.
9. Orsini JJ, et al. Newborn screening for Krabbe disease in New York State: the first eight years' experience. *Genet Med*. 2016;18(3):239–248.
10. Victoria T, Rafi MA, Wenger DA. Cloning of the canine GALC cDNA and identification of the mutation causing globoid cell leukodystrophy in West Highland White and Cairn terriers. *Genomics*. 1996;33(3):457–462.
11. Bradbury A, Peterson D, Vite C, Chen S, Ellinwood NM, Provenzale J. Diffusion tensor imaging analysis of the brain in the canine model of Krabbe disease. *Neuroradiol J*. 2016;29(6):417–424.
12. Bradbury AM, et al. Clinical, electrophysiological, and biochemical markers of peripheral and central nervous system disease in canine globoid cell leukodystrophy (Krabbe's disease). *J Neurosci Res*. 2016;94(11):1007–1017.
13. Cozzi F, Vite CH, Wenger DA, Victoria T, Haskins ME. MRI and electrophysiological abnormalities in a case of canine globoid cell leucodystrophy. *J Small Anim Pract*. 1998;39(8):401–405.
14. Wenger DA, et al. Globoid cell leukodystrophy in cairn and West Highland white terriers. *J Hered*. 1999;90(1):138–142.
15. Karumuthil-Melethil S, Marshall MS, Heindel C, Jakubauskas B, Bongarzone ER, Gray SJ. Intrathecal administration of AAV/GALC vectors in 10-11-day-old twitcher mice improves survival and is enhanced by bone marrow transplant. *J Neurosci Res*. 2016;94(11):1138–1151.
16. Corado CR, et al. Cerebrospinal fluid and serum glycosphingolipid biomarkers in canine globoid cell leukodystrophy (Krabbe Disease). *Mol Cell Neurosci*. 2020;102:103451.
17. Bradbury AM, et al. AAVrh10 gene therapy ameliorates central and peripheral nervous system disease in canine globoid cell leukodystrophy (Krabbe disease). *Hum Gene Ther*. 2018;29(7):785–801.
18. Wu YP, McMahon EJ, Matsuda J, Suzuki K, Matsushima GK, Suzuki K. Expression of immune-related molecules is downregulated in twitcher mice following bone marrow transplantation. *J Neuropathol Exp Neurol*. 2001;60(11):1062–1074.
19. Reddy AS, et al. Bone marrow transplantation augments the effect of brain- and spinal cord-directed adeno-associated virus 2/5 gene therapy by altering inflammation in the murine model of globoid-cell leukodystrophy. *J Neurosci*. 2011;31(27):9945–9957.
20. Schuster DJ, et al. Biodistribution of adeno-associated virus serotype 9 (AAV9) vector after intrathecal and intravenous delivery in mouse. *Front Neuroanat*. 2014;8:42.
21. Hordeaux J, et al. Safe and sustained expression of human iduronidase after intrathecal administration of adeno-associated virus serotype 9 in infant rhesus monkeys. *Hum Gene Ther*. 2019;30(8):957–966.
22. Hinderer C, et al. Severe toxicity in nonhuman primates and piglets following high-dose intravenous administration of an adeno-associated virus vector expressing human SMN. *Hum Gene Ther*. 2018;29(3):285–298.
23. Gray SJ, Nagabhushan Kalburgi S, McCown TJ, Jude Samulski R. Global CNS gene delivery and evasion of anti-AAV-neutralizing antibodies by intrathecal AAV administration in non-human primates. *Gene Ther*. 2013;20(4):450–459.
24. Gray SJ, Matagne V, Bachaboina L, Yadav S, Ojeda SR, Samulski RJ. Preclinical differences of intravascular AAV9 delivery to neurons and glia: a comparative study of adult mice and nonhuman primates. *Mol Ther*. 2011;19(6):1058–1069.
25. Suzuki K, Suzuki K. The twitcher mouse: a model for Krabbe disease and for experimental therapies. *Brain Pathol*. 1995;5(3):249–258.
26. Sakai N, et al. Molecular cloning and expression of cDNA for murine galactocerebrosidase and mutation analysis of the twitcher mouse, a model of Krabbe's disease. *J Neurochem*. 1996;66(3):1118–1124.
27. Ohno K, et al. Kinetics and MR-based monitoring of AAV9 vector delivery into cerebrospinal fluid of nonhuman primates. *Mol Ther Methods Clin Dev*. 2019;13:47–54.
28. Madsen AMH, Wibrand F, Lund AM, Ek J, Dunø M, Østergaard E. Genotype and phenotype classification of 29 patients affected by Krabbe disease. *JIMD Rep*. 2019;46(1):35–45.
29. Tappino B, et al. Identification and characterization of 15 novel GALC gene mutations causing Krabbe disease. *Hum Mutat*. 2010;31(12):E1894–E1914.
30. Escolar ML, et al. Psychosine, a marker of Krabbe phenotype and treatment effect. *Mol Genet Metab*. 2017;121(3):271–278.
31. Langan TJ, et al. Development of a newborn screening tool based on bivariate normal limits: using psychosine and galactocerebrosidase determination on dried blood spots to predict Krabbe Disease. *Genet Med*. 2019;21(7):1644–1651.
32. Golebiowski D, et al. Direct intracranial injection of AAVrh8 encoding monkey β-N-acetylhexosaminidase causes neurotoxicity in the primate brain. *Hum Gene Ther*. 2017;28(6):510–522.
33. Sural-Fehr T, et al. Inhibition of the IGF-1-PI3K-Akt-mTORC2 pathway in lipid rafts increases neuronal vulnerability in a genetic lysosomal glycosphingolipidosis. *Dis Model Mech*. 2019;12(5):dmm036590.
34. Poretti A, et al. Novel diffusion tensor imaging findings in Krabbe disease. *Eur J Paediatr Neurol*. 2014;18(2):150–156.
35. Sasaki M, Sakuragawa N, Takashima S, Hanaoka S, Arima M. MRI and CT findings in Krabbe disease. *Pediatr Neurol*. 1991;7(4):283–288.
36. Murlidharan G, Crowther A, Reardon RA, Song J, Asokan A. Glymphatic fluid transport controls paravascular clearance of AAV vectors from the brain. *JCI Insight*. 2016;1(14):e88034.
37. Duffner PK, et al. The long-term outcomes of presymptomatic infants transplanted for Krabbe disease: report of the workshop held on July 11 and 12, 2008, Holiday Valley, New York. *Genet Med*. 2009;11(6):450–454.
38. Siddiqi ZA, Sanders DB, Massey JM. Peripheral neuropathy in Krabbe disease: effect of hematopoietic stem cell transplantation. *Neurology*. 2006;67(2):268–272.
39. Gurda BL, et al. Evaluation of AAV-mediated gene therapy for central nervous system disease in canine Mucopolysaccharidosis VII. *Mol Ther*. 2016;24(2):206–216.
40. McCabe JS, Low FN. The subarachnoid angle: an area of transition in peripheral nerve. *Anat Rec*. 1969;164(1):15–33.
41. Kagiava A, Kleopa KA. Intrathecal delivery of viral vectors for gene therapy. *Methods Mol Biol*. 2018;1791:277–285.
42. Kagiava A, et al. Intrathecal gene therapy rescues a model of demyelinating peripheral neuropathy. *Proc Natl Acad Sci U S A*. 2016;113(17):E2421–E2429.
43. Hennig AK, et al. Intravitreal gene therapy reduces lysosomal storage in specific areas of the CNS in mucopolysaccharidosis VII mice. *J Neurosci*. 2003;23(8):3302–3307.
44. Griffey M, Macauley SL, Ogilvie JM, Sands MS. AAV2-mediated ocular gene therapy for infantile neuronal ceroid lipofuscinosis. *Mol Ther*. 2005;12(3):413–421.
45. Clément N, Grieger JC. Manufacturing of recombinant adeno-associated viral vectors for clinical trials. *Mol Ther Methods Clin Dev*. 2016;3:16002.
46. Gray SJ, Choi VW, Asokan A, Haberman RA, McCown TJ, Samulski RJ. Production of recombinant adeno-associated viral vectors and use in in vitro and in vivo administration. *Curr Protoc Neurosci*. 2011;57(1):4.17.1–4.17.30.
47. Marshall MS, et al. Long-term improvement of neurological signs and metabolic dysfunction in a mouse model of Krabbe's disease after global gene therapy. *Mol Ther*. 2018;26(3):874–889.
48. Sidhu R, et al. A HILIC-MS/MS method for simultaneous quantification of the lysosomal disease markers galactosylsphingosine and glucosylsphingosine in mouse serum. *Biomed Chromatogr*. 2018;32(7):e4235.